

Supporting Information for

Atmospheric response to oceanic cold eddies west of Luzon in the northern South China Sea

Haoya LIU, Shumin CHEN*, Weibiao LI, Rong FANG, Zhuo LI, and Yushi Wu

School of Atmospheric Sciences, Sun Yat-Sen University, Guangzhou 510275, China

For submission to:

Atmosphere

6-May-2019

*Correspondence:

Shumin CHEN

School of Atmospheric Sciences, Sun Yat-Sen University, Guangzhou 510275, China.

Email: es04csm@mail2.sysu.edu.cn

Contents of this file

Text S1

Text S2

Text S3

Text S4

Text S5

Figure S1

Figure S2

Figure S3

Figure S4

Figure S5

Figure S6

***Correspondence:** S. Chen, School of Atmospheric Sciences, Sun Yat-Sen University, Guangzhou 510275, China.

Email: es04csm@mail2.sysu.edu.cn

Funding information: the National Natural Science Foundation of China (Grant Nos. 41675043 and 41375050).

Contents

Text S1:

Overall, 1521 eddy records with amplitude >4 cm were used in the composite maps, which correspond to 12 central type LCEs (comprising 840 eddy records) and 8 peripheral type LCEs (comprising 681 eddy records). Figure s1 shows the variability of size and amplitude for eddies that go into the composites. As shown in Figure s1, more than 90% of eddy records were larger than 70 km and stronger than 5 cm; and about 80% of eddy records in the composite analyses have radii between 70 and 120 km and amplitudes between 5 and 16 cm.

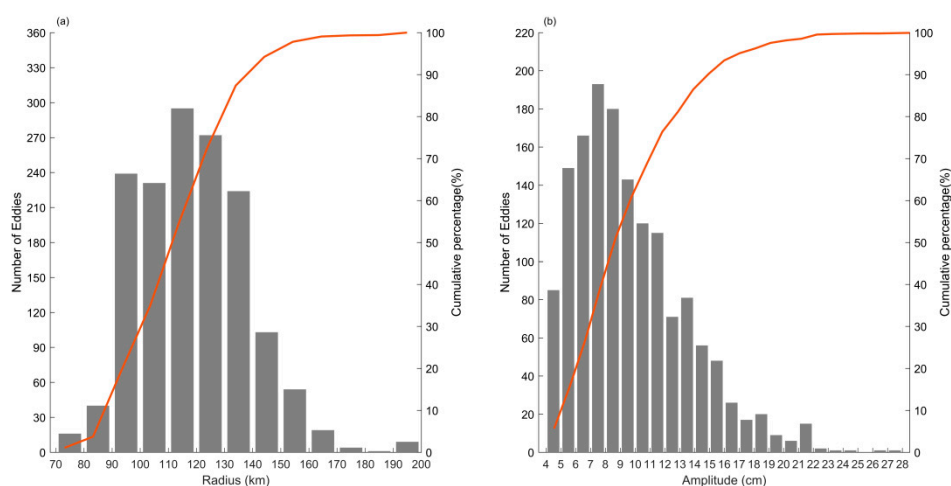


Figure S1. Histograms and cumulative probability (red line) of eddy radius **(a)** and amplitude **(b)** for 1521 eddy records that were used in the composite maps.

Text S2:

Turbulent heat flux anomalies related to LCEs are also examined by the IFREMER and J-OFURO datasets. The spatial resolution of IFREMER and J-OFURO heat flux datasets is 0.25° latitude by 0.25° longitude which is much higher than the OA Flux dataset (1° resolution). Daily latent heat flux and sensible heat flux from IFREMER are provided from October 1999 to November 2009. Thus, the date range for IFREMER is much shorter than the OA Flux, only 11 LCEs (comprising 534 eddy records for central type LCEs and 302 eddy records for peripheral type LCEs) are included. The high-resolution J-OFURO dataset is available from 2000 to 2013 which covered 17 LCEs (comprising 643 eddy

records for central type LCEs and 583 eddy records for peripheral type LCEs).

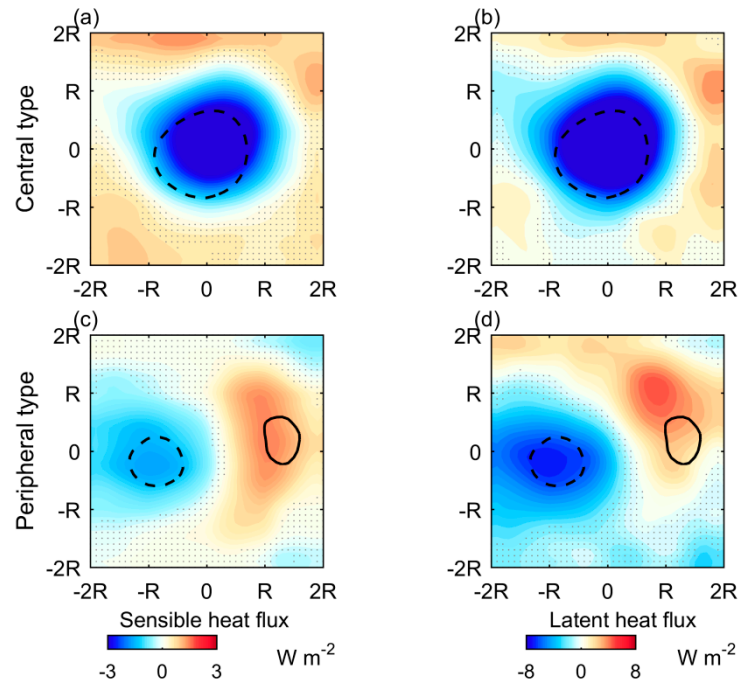


Figure S2. As Figure 3 (c, g) and (d, h), but based on IFREMER dataset. Composition of SHF anomalies and LHF anomalies based on 11 LECs during 2000 to 2009.

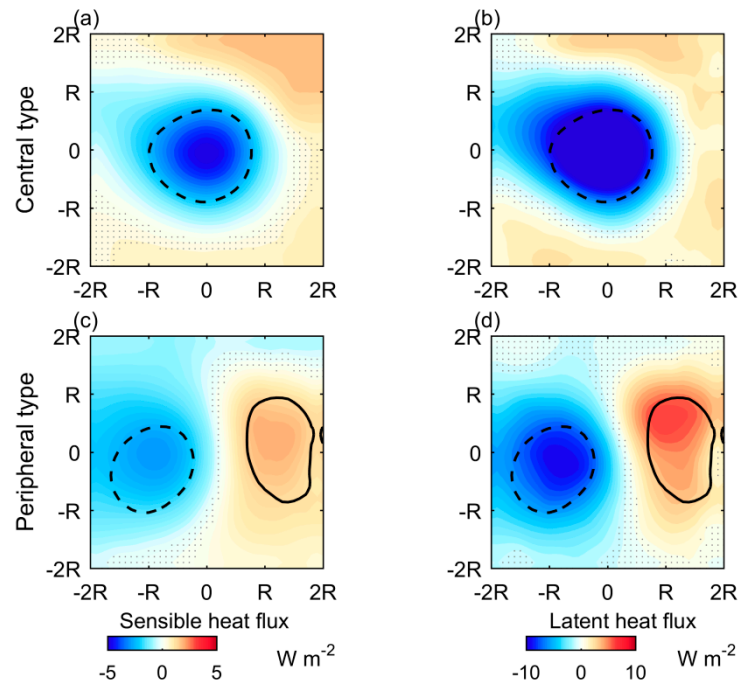


Figure S3. As Figure 3 (c, g) and (d, h), but based on J-OFURO dataset. Composition of SHF anomalies and LHF anomalies based on 17 LECs during 2000 to 2013.

Text S3:

The sea level pressure (SLP) obtained from the CFSR reanalysis data was employed here (<https://rda.ucar.edu/datasets/ds093.0/>). As shown in Figure S4, the SLP is increased over the cold water and decreased over the warm water. However, these SLP anomalies associated with LCEs are not statistically significant.

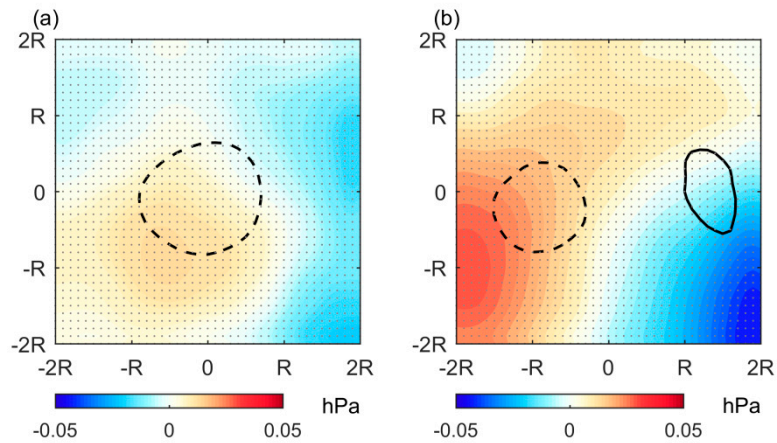


Figure S4. Same as Figure 5, but for sea level pressure (SLP) anomalies. Areas with dots are NOT significantly different from zero at the 99% confidence level based on a t-test.

Text S4:

A schematic diagram is given in Figure S5 to show the thermodynamical and dynamical adjustment processes in eddy-related rain rate modification.

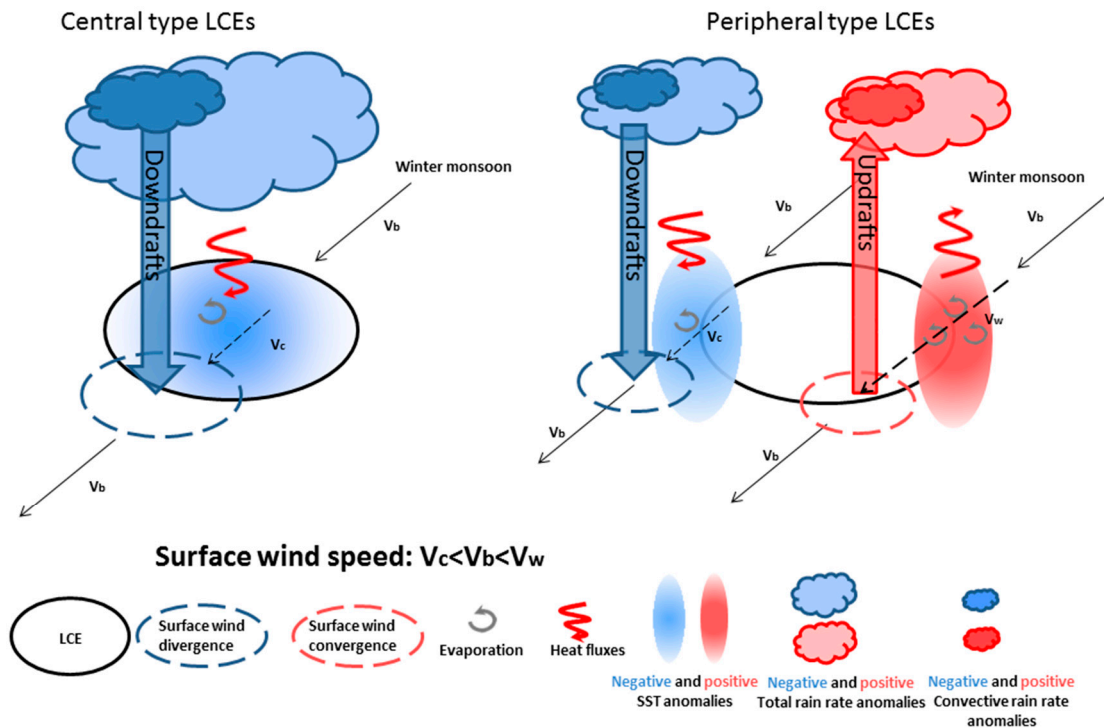


Figure S5. Impact of Luzon cold eddies on the local rain rate. Schematic summarizing the impact of central type LCEs (left) and peripheral type LCEs (right) on the total rain rate and the convective rain rate. The total rain rate anomalies are close in phase to SST anomalies, which points to a modification of the atmospheric stability in combination with changes in turbulent heat fluxes and evaporations. The convective rain rate anomalies are 90° out of phase to SST anomalies, which points to a modification of vertical motion caused by anomalous surface wind divergence.

Text S5:

Scatter diagram of the prefiltered curl of the ocean surface current against the prefiltered curl of the atmospheric wind is shown as Figure S6. The effect of the ocean current driving the atmosphere failed the test of significance. Thus, the “ocean surface current feedback to the atmosphere” as pointed out by Renaud et al. [1] seems not statistically significant for LCEs.

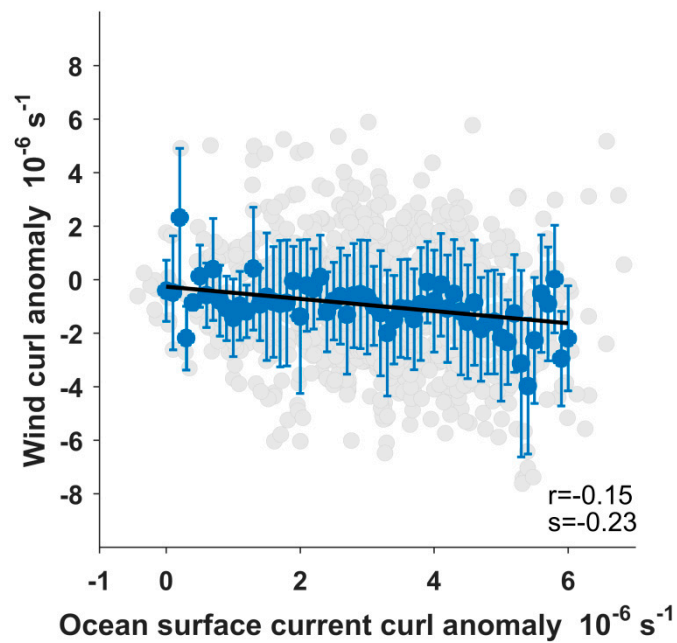


Figure S6. Binned scatterplot of the curl of the ocean surface current against the curl of the atmospheric wind, including 1521 eddy records correspond to all 20 LCEs. Prefiltered data were used to reveal scales associated with the LCEs. The effect of the ocean current driving the atmosphere failed the test of significance (correlation coefficient (r) and the slope (s) are listed in the figure).

Reference:

1. Renault, L.; Molemaker, M.J.; McWilliams, J.C.; Shchepetkin, A.; Florian, L.; Chelton, D.; Illig, S.; Hall, A. Modulation of wind-work by oceanic current interaction with the atmosphere. *J. Phys. Oceanogr.* **2016**, *46*(6), 1685–1704.